

Al-Nb-Ti (Aluminum-Niobium-Titanium)

V. Raghavan

This ternary system was reviewed earlier by [1993Gam], who presented a liquidus projection, experimental isothermal sections at 1200, 1100, and 1000 °C, computed isothermal sections from [1992Kat] at 1400, 1200, 1100, and 700 °C, and a vertical section along the NbAl₃-TiAl₃ join. More recent results were reviewed in the update by [2005Rag]. At about the same time, an update of the review of [1993Gam] was presented by [2005Tre]. Very recently, two detailed thermodynamic assessments of this system [2009Cup, 2009Wit] have been carried out. In addition, [2009Wit] reported new experimental results, which were included in their optimization.

and TiAl₃ (LT) tetragonal, space group *I4/mmm*, denoted ϵ (l) by [2009Wit]). Based on the assessment of [2008Wit], [2009Wit] included two previously known compounds: Ti_{2+x}Al_{5-x} (tetragonal, space group *P4/mmm*, denoted ζ) and Ti₃Al₅ (Ti₃Ga₅-type tetragonal, space group *P4/mbm*). These were excluded by [2006Sch] in their assessed diagram. There are no intermediate phases in the Nb-Ti phase diagram [1994Har]. Nb and β Ti form a continuous bcc solid solution. The β Ti \rightarrow α Ti transformation temperature is lowered by the addition of Nb.

Binary Systems

The Al-Nb phase diagram re-determined by [2009Wit] is shown in Fig. 1. It depicts three intermediate phases with significant ranges of homogeneity: Nb₃Al (*A15*, Cr₃Si-type cubic, labeled δ), Nb₂Al (*D8_b*, σ CrFe-type tetragonal labeled σ), and NbAl₃ (*D0₂₂*, TiAl₃(HT)-type tetragonal, denoted ϵ). The Al-Ti phase diagram [2006Sch] has the following intermediate phases: Ti₃Al (*D0₁₉*, Ni₃Sn-type hexagonal, denoted α_2), TiAl (*L1₀*, AuCu-type tetragonal, denoted γ), TiAl₂ (HfGa₂-type tetragonal, denoted η by [2009Wit] and ϵ by [2009Cup]), TiAl₃ (HT) (*D0₂₂*-type tetragonal, denoted ϵ by [2009Wit] and η by [2009Cup]),

Ternary Phases

A NaHg-type orthorhombic phase denoted O, first reported by [1988Ban], occurs at the nominal composition Ti₂NbAl, with the lattice parameters of $a = 0.60983$ nm, $b = 0.95694$ nm and $c = 0.46666$ nm. The O-phase undergoes an ordering transformation, with preference for site occupancies between Nb and Ti atoms [2001Ser, 2008Wu]. [2008Wu] concluded that the order-disorder transformation is a second-order transition. However, following [1998Ser], [2009Wit] assumed two distinct phases O₁ and O₂, both of the NaHg-type but with different site occupancies. According to their computed reaction sequence, the O₁ phase forms at a peritectic maximum at 996 °C and decomposes through a ternary eutectoid reaction at 843 °C. The O₂ phase forms through a ternary peritectic reaction at 923 °C and is stable at lower temperatures. The first-order transitions implied in the description of [2009Wit] appear doubtful. Further, in a subsequent publication, [2001Ser] modeled the orthorhombic phase with a continuous function, comprised of order-dependent and order-independent terms.

A second ternary phase Ti₄NbAl₃ (denoted τ) forms at a peritectic maximum at 811 °C and is stable down to room temperature [2005Rag, 2009Wit]. It has the *B8₂*-type hexagonal structure. There has been no confirmation of a third ternary phase TiNbAl₃ labeled γ_1 reported by [1994Wan].

Thermodynamic Descriptions

In the thermodynamic description, [2009Wit] modeled the liquid, fcc, bcc and cph phases as substitutional solutions. An ordering energy term was added to the bcc description to describe the *B2* ordering. The binary phases with ternary solubility were described with appropriate sublattice models. The O₁ and O₂ ternary phases were described with two and three sublattices respectively. The ternary phase Ti₄NbAl₃ (τ) was taken as a stoichiometric compound. The established binary descriptions from the literature were used. In the optimization, [2009Wit] used selected data from phase

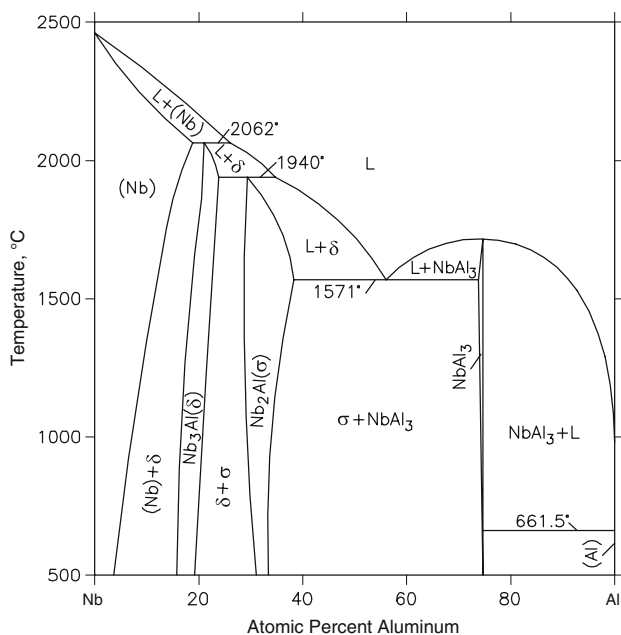


Fig. 1 Al-Nb binary phase diagram [2009Wit]

Section II: Phase Diagram Evaluations

equilibria and thermodynamic properties from the literature supplemented with their own measurements. The optimized interaction parameters were listed.

In their thermodynamic description, [2009Cup] modeled the liquid, fcc, bcc and cph phases as substitutional solutions. The binary phases with ternary solubility were described with sublattice models. The ternary phases σ and τ were omitted. Their calculations do not extend to the range below 1000 °C, where these phases are stable. A single Gibbs energy function was used to describe the disordered and ordered states of $\text{bcc} \leftrightarrow B2$ and $\alpha \leftrightarrow \alpha_2$ transitions. [2009Cup] listed the key experimental data on the ternary system from the literature, indicating those which were employed in the optimization. The optimized interaction parameters were listed.

Liquidus and Solidus Projections

With starting metals of 99.99% Al, 99.9% Nb and 99.9% Ti, [2009Wit] arc-melted under Ar atm 26 ternary alloys with Nb contents ranging between 4 and 19 at.%. As-cast and annealed samples were characterized with optical and scanning electron microscopy, energy dispersive spectroscopy, x-ray powder diffraction and differential thermal analysis at heating/cooling rates of 20 or 40 °C per min. The observed thermal arrests for the various alloys were listed together with the calculated values from the thermodynamic description. Also, the standard enthalpy of formation of one ternary alloy $\text{Ti}_{25.3}\text{Nb}_{19.0}\text{Al}_{55.7}$ (γ) was measured by drop isoperibolic calorimetry. [2009Cup] did not carry out any new experiments.

The liquidus projections computed by [2009Wit] and [2009Cup] are compared in Fig. 2. The overall agreement is

satisfactory. A significant difference is in the extent of the primary crystallization region of bcc (Nb, β Ti). [2009Wit] pointed out that, as compared to the previous thermodynamic assessments of [1992Kat] and [2001Ser], their results show that the primary crystallization region of bcc extends more towards Al-rich compositions. However, as seen in Fig. 2, the results of [2009Cup] show the region extending to even higher Al contents as compared to the results of [2009Wit]. [2009Cup] supported their results with selected experimental data from [1992Fen], [2000Leo] and [2009Rio] shown in Fig. 2. These data were used in the optimization by [2009Cup], whereas [2009Wit] did not list the data they used in the optimization. Also, [2009Wit] did not list the two references of [1992Fen] and [2009Rio]. Clearly, more experimental results are needed to resolve this point in the composition region of ~30-50 at.% Al and ~10-40 at.% Ti. The solidus projections computed by [2009Wit] and [2009Cup] are compared in Fig. 3. The overall agreement is satisfactory.

Isothermal and Vertical Sections

From their thermodynamic model, [2009Wit] computed 12 isothermal sections at 1650, 1400, 1200, 1150, 1100, 1060, 1000, 900, 800, 700, 600 and 25 °C. The sections were compared with a large amount of experimental data from the literature and their own results. The overall agreement is satisfactory. [2009Cup] computed seven isothermal sections at 1650, 1540, 1400, 1300, 1200, 1100 and 1000 °C and compared them with experimental data both included and excluded in the optimization. The overall agreement is satisfactory. Figure 4 compares the computed

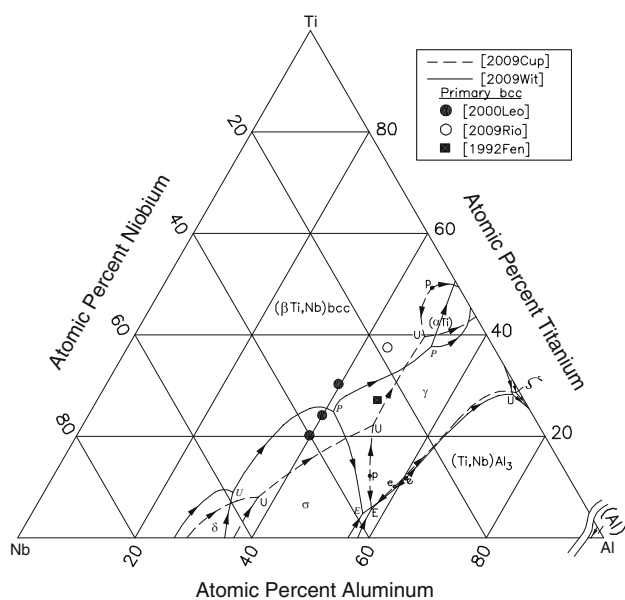


Fig. 2 Al-Nb-Ti computed liquidus projection [2009Cup, 2009Wit]

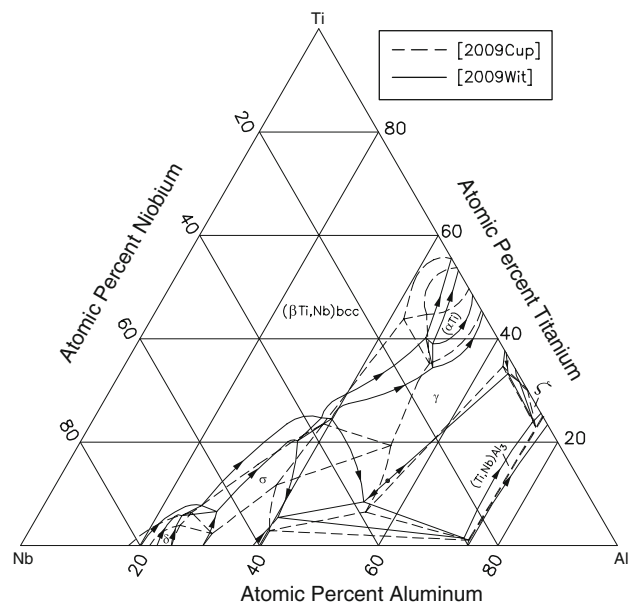


Fig. 3 Al-Nb-Ti computed solidus projection [2009Cup, 2009Wit]

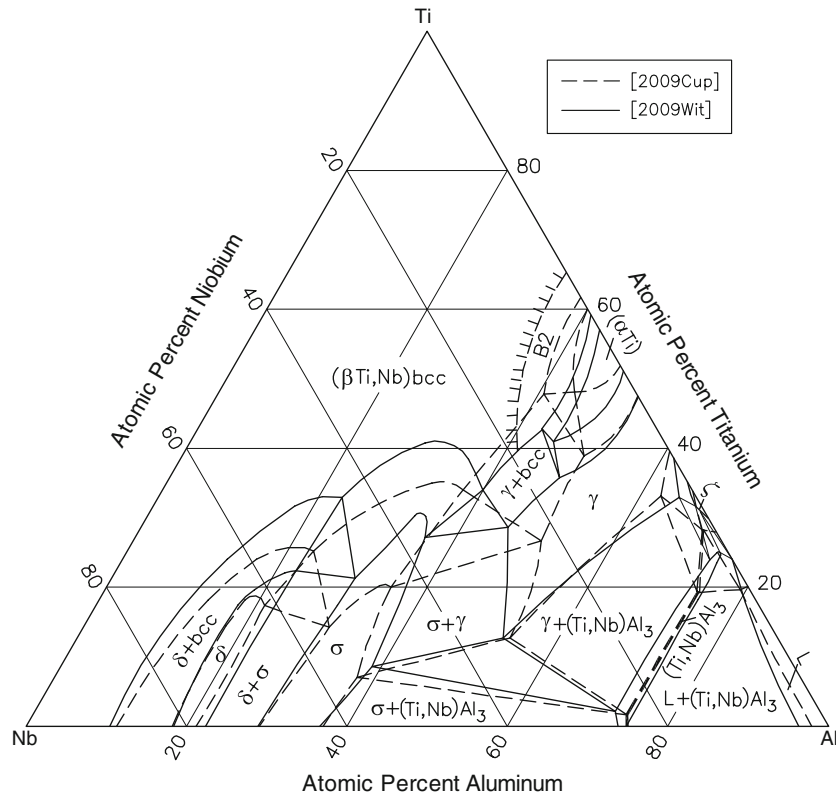


Fig. 4 Al-Nb-Ti computed isothermal section at 1400 °C [2009Cup, 2009Wit]

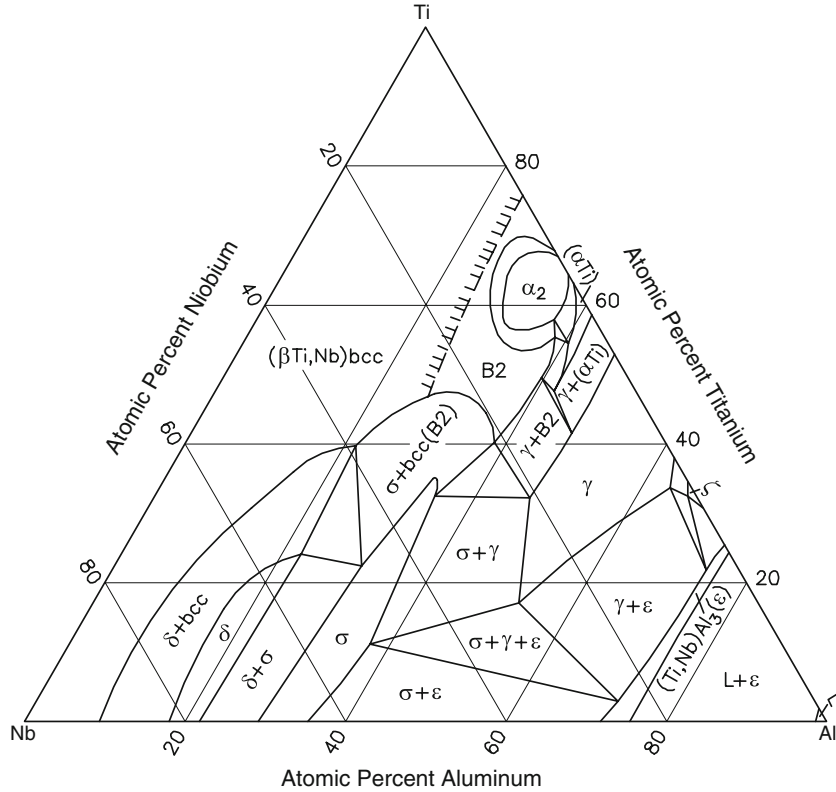


Fig. 5 Al-Nb-Ti computed isothermal section at 1200 °C [2009Wit]

Section II: Phase Diagram Evaluations

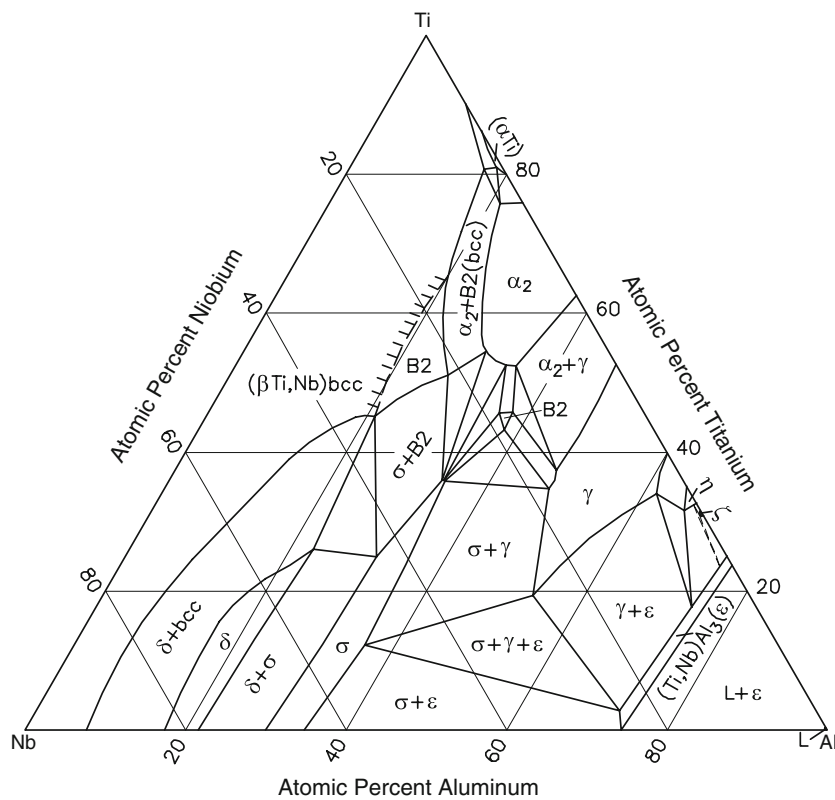


Fig. 6 Al-Nb-Ti computed isothermal section at 1000 °C [2009Wit]

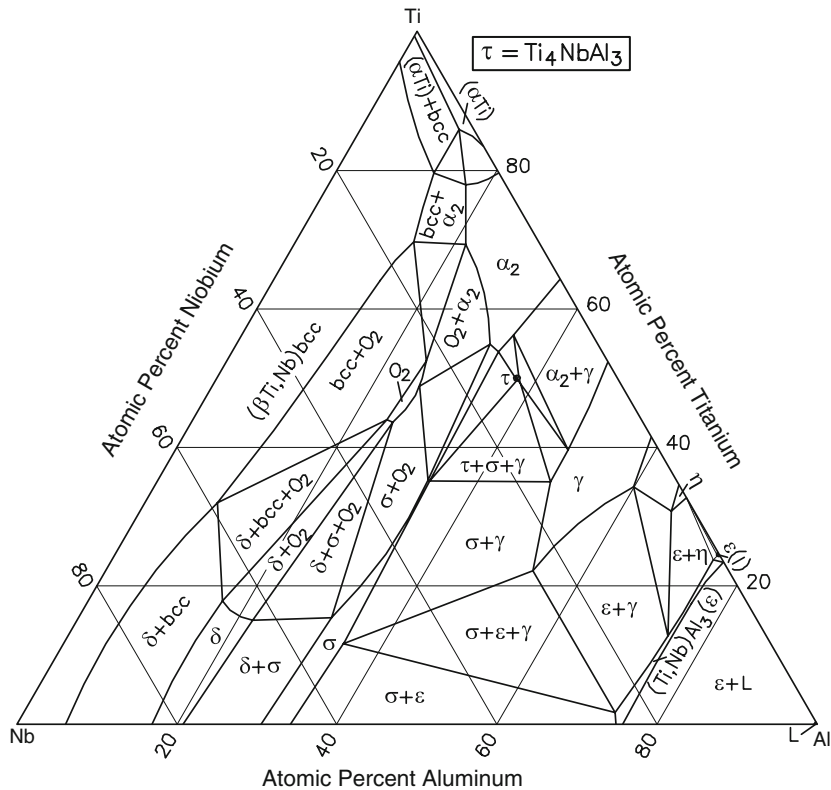


Fig. 7 Al-Nb-Ti computed isothermal section at 800 °C [2009Wit]

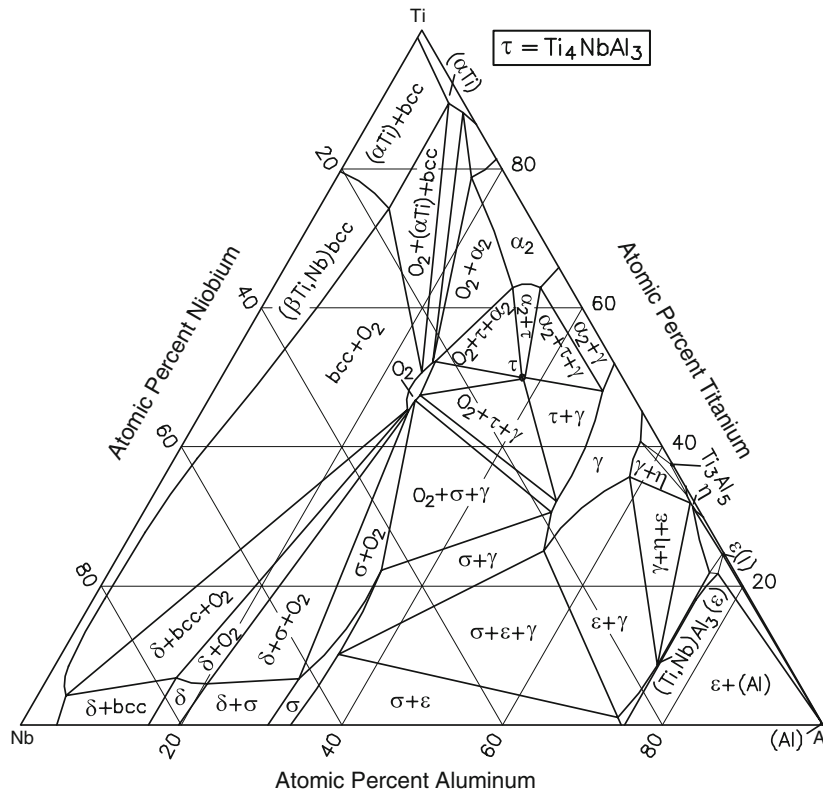


Fig. 8 Al-Nb-Ti computed isothermal section at 600 °C [2009Wit]

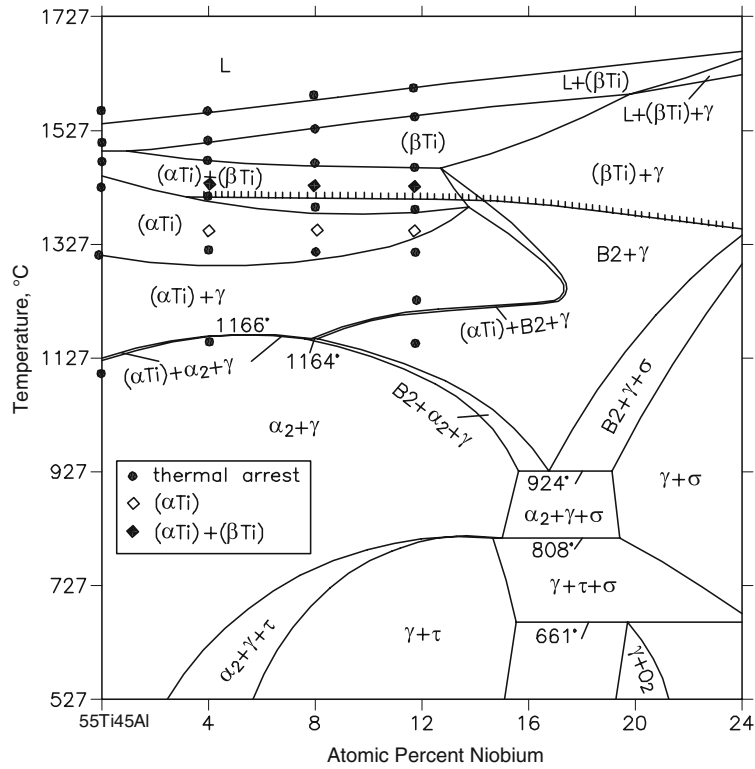


Fig. 9 Al-Nb-Ti computed vertical section along $Ti_{55}Al_{45}-Ti_{29}Nb_{24}Al_{47}$ join [2009Wit]

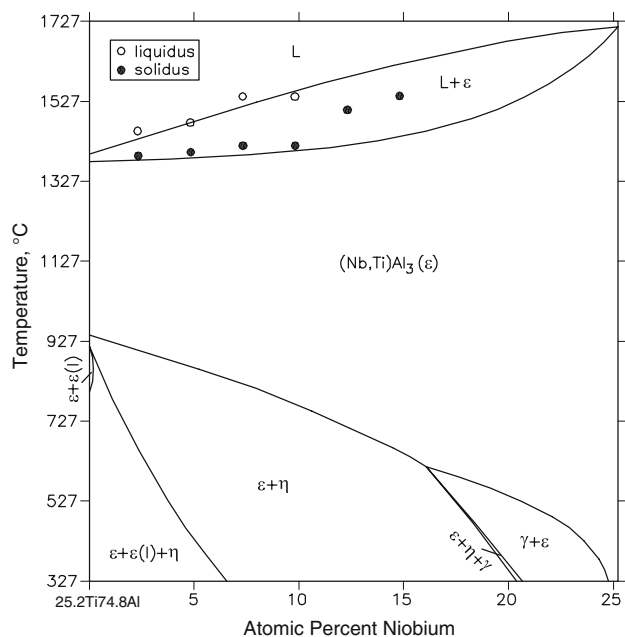


Fig. 10 Al-Nb-Ti computed vertical section along $Ti_{25.2}Al_{74.8}$ - $Nb_{25.2}Al_{74.8}$ join [2009Wit]

isothermal sections of [2009Wit] and [2009Cup] at 1400 °C. To preserve clarity, the experimental tie-lines are not shown. The experimental δ -bcc tie-lines from [1990Per] and [1998Wan] were found to fall to the left of the (δ + bcc) two-phase field. Figures 5-8 show the isothermal sections computed by [2009Wit] at 1200, 1000, 800 and 600 °C respectively. For clarity, the experimental tie-lines are omitted. The nucleation of η at a peritectoidal maximum on the ζ - γ tie-line at 1257 °C [2009Wit] would replace the ζ + γ + ε tie-triangle in Fig. 5 with three triangles of η + γ + ζ , η + γ + ε and η + ζ + ε . To preserve clarity, this feature is not shown in Fig. 5 (1200 °C). At 1000 °C (Fig. 6), a separate island of B2 has nucleated at the eutectoidal maximum on the α_2 - σ tie-line at 1073 °C [2009Wit]. At 800 °C (Fig. 7), the O_2 phase is present. The low-temperature form of $TiAl_3$, $\varepsilon(l)$, which has nucleated at 932 °C, coexists with the high-temperature form ε [2009Wit]. The τ phase is stable due to its formation at a peritectoidal maximum of 819 °C along the α_2 + γ tie-line [2009Wit]. At 600 °C (Fig. 8), the last liquid at the Al corner has solidified to (Al).

[2009Wit] computed eight vertical sections and compared them with experimental data. The agreement was found to be satisfactory. As examples, two vertical sections along $Ti_{55}Al_{45}$ - $Ti_{29}Nb_{24}Al_{47}$ and $Ti_{25.2}Al_{74.8}$ - $Nb_{25.2}Al_{74.8}$ joins are shown in Fig. 9 and 10. The invariant horizontals at 1164, 924, 808 and 661 °C in Fig. 9 correspond to the following reactions in the reaction table of [2009Wit]: (αTi) \leftrightarrow α_2 + B2 + γ (labeled Ed₁ by [2009Wit]), B2 \leftrightarrow α_2 + γ + σ (labeled Ed₂), α_2 + γ \leftrightarrow σ + τ (labeled Ud₆) and σ + τ \leftrightarrow γ + O_2 (labeled Ud₈) respectively. Figure 10 depicts the pseudobinary character of the solidification of (Nb,Ti)Al₃ along $TiAl_3$ - $NbAl_3$ join at a slightly off-stoichiometric composition.

References

- 1988Ban:** B. Banerjee, A.K. Gogia, T.K. Nandi, and V.A. Joshi, A New Ordered Orthorhombic Phase in a Ti_3Al -Nb Alloy, *Acta Metall.*, 1988, **36**(4), p 871-882
- 1990Per:** J.H. Perepezko, Y.A. Chang, L.E. Seitzman, J.C. Lin, N.R. Bonda, T.J. Jewett, and J.C. Mishurda, High Temperature Phase Stability in the Ti-Al-Nb System, *High Temperature Aluminides Intermetallics Proceedings Symposium*, 1989, S.H. Wang, Ed., The Minerals, Metals & Materials Society, Warrendale, PA, 1990, p 19-47
- 1992Fen:** C.R. Feng and D.J. Michel, Microstructure of Nb-26Ti-48Al + (Nb,Ti)B, *Mater. Sci. Eng. A*, 1992, **152**, p 202-207
- 1992Kat:** U.R. Kattner and W.J. Boettinger, Thermodynamic Calculation of the Ternary Ti-Al-Nb System, *Mater. Sci. Eng. A*, 1992, **152**, p 9-17
- 1993Gam:** S. Gama, Aluminum-Niobium-Titanium, *Ternary Alloys*, Vol 7, G. Petzow and G. Effenberg, Ed., VCH Verlagsgesellschaft, Weinheim, Germany, 1993, p 382-398
- 1994Har:** K.C. Hari Kumar, P. Wollants, and L. Delaey, Thermodynamic Calculation of Nb-Ti-V Phase Diagram, *CALPHAD*, 1994, **18**(1), p 71-79
- 1994Wan:** J. Wang, G. Chen, Z. Sun, and Y. He, Phase Relations in TiAl + Nb System, *J. Mater. Sci. Technol. Shenyang*, 1994, **10**(5), p 359-366
- 1998Ser:** C. Servant and I. Ansara, Thermodynamic Assessment of the Al-Nb-Ti System, *Ber. Bunsenges. Phys. Chem.*, 1998, **102**(9), p 1189-1205
- 1998Wan:** X.T. Wang, G.L. Chen, K.Q. Ni, and S.M. Hao, The 1400 °C Isothermal Section of the Ti-Al-Nb Ternary System, *J. Phase Equilib.*, 1998, **19**(3), p 200-205
- 2000Leo:** K.J. Leonard, J.C. Mishurda, and V.K. Vasudevan, Examination of Solidification Pathways and the Liquidus Surface in the Nb-Ti-Al System, *Metall. Mater. Trans. B*, 2000, **31**, p 1305-1321
- 2001Ser:** C. Servant and I. Ansara, Thermodynamic Modeling of the Order-Disorder Transformation of the Orthorhombic Phase of the Al-Nb-Ti System, *CALPHAD*, 2001, **25**, p 509-525
- 2005Rag:** V. Raghavan, Al-Nb-Ti (Aluminum-Niobium-Titanium), *J. Phase Equilib. Diffus.*, 2005, **26**(4), p 360-368
- 2005Tre:** L. Tretyachenko, Aluminum-Niobium-Titanium, *Landolt-Bornstein New Series IV*, Vol 11A3, G. Effenberg and S. Ilyenko, Ed., 2005, p 334-379
- 2006Sch:** J.C. Schuster and M. Palm, Reassessment of the Binary Aluminum-Titanium Phase Diagram, *J. Phase Equilib. Diffus.*, 2006, **27**(3), p 255-277
- 2008Wit:** V.T. Witusiewicz, A.A. Bondar, U. Hecht, S. Rex, and T.Ya. Velikanova, The Al-B-Nb-Ti System III. Thermodynamic Reevaluation of the Constituent Binary System Al-Ti, *J. Alloys Compd.*, 2008, **456**, p 64-77
- 2008Wu:** B. Wu, M. Zinkevich, F. Aldinger, M. Chu, and J. Shen, Prediction of the Ordering Behaviors of the Orthorhombic Phase Based on Ti_2AlNb Alloys by Combining Thermodynamic Model with *ab initio* Calculation, *Intermetallics*, 2008, **16**, p 42-51
- 2009Cup:** D.M. Cupid, O. Fabrichnaya, O. Rios, F. Ebrahimi, and H.J. Seifert, Thermodynamic Re-assessment of the Ti-Al-Nb System, *Int. J. Mater. Res.*, 2009, **100**(2), p 218-233
- 2009Rio:** O. Rios, S. Goyel, M.S. Kesler, D.M. Cupid, H.J. Seifert, and F. Ebrahimi, An Evaluation of High-Temperature Phase Stability in the Ti-Al-Nb System, *Scr. Mater.*, 2009, **60**, p 156-159
- 2009Wit:** V.T. Witusiewicz, A.A. Bondar, U. Hecht, and T.Ya. Velikanova, The Al-B-Nb-Ti System IV. Experimental Study and Thermodynamic Reevaluation of the Binary System Al-Nb and Al-Nb-Ti Systems, *J. Alloys Compd.*, 2009, **472**, p 133-161